



# Microstructural features of parapapillary gamma zone and beta zone in non-myopic eyes

Kunte Shang<sup>1,2#</sup>, Dongli Zhuang<sup>1,2#</sup>, Yi Dai<sup>1,2</sup>

<sup>1</sup>Department of Ophthalmology & Visual Science, Eye & ENT Hospital, Shanghai Medical College, Fudan University, Shanghai, China; <sup>2</sup>NHC Key Laboratory of Myopia (Fudan University), Key Laboratory of Myopia, Chinese Academy of Medical Sciences, and Shanghai Key Laboratory of Visual Impairment and Restoration (Fudan University), Shanghai, China

*Contributions:* (I) Conception and design: Y Dai; (II) Administrative support: Y Dai; (III) Provision of study materials or patients: Y Dai; (IV) Collection and assembly of data: K Shang, D Zhuang; (V) Data analysis and interpretation: K Shang, D Zhuang; (VI) Manuscript writing: All authors; (VII) Final approval of manuscript: All authors.

<sup>#</sup>These authors contributed equally to this work.

*Correspondence to:* Yi Dai, MD, PhD. Department of Ophthalmology, Eye & ENT Hospital, Fudan University, 83 Fenyang Road, Shanghai 200031, China. Email: ydai@fudan.edu.cn.

**Background:** To investigate the microstructural features of parapapillary gamma zone and beta zone and their relationship with three-dimensional optic disc shape in non-myopic eyes.

**Methods:** This cross-sectional study included 62 non-myopic eyes with parapapillary gamma or beta zone and 70 control eyes. On the spectral domain optical coherent tomography (SD-OCT) images, we measured the area of gamma zone and beta zone, the length of border tissue, and related disc parameters. The disc ovality index, disc rotation degrees around three axes, Bruch's membrane opening (BMO) ovality ratio were calculated based on the SD-OCT images.

**Results:** The parapapillary gamma zone composed by externally oblique border tissue was found in inferior, nasal and temporal quadrants of the non-myopic eyes. The presence of gamma zone in non-myopic eyes was correlated with smaller disc ovality index, larger rotation degree around vertical and horizontal axes, and larger BMO ovality ratio ( $P < 0.001$ ). Compared with the non-temporal gamma zone group, eyes with temporal gamma zone had a longer axial length and rotated more around vertical axes ( $P < 0.001$ ). Multivariate analysis showed that the area of gamma zone was correlated with the disc ovality index ( $P < 0.001$ ). The presence and area of beta zone was correlated with age ( $P < 0.01$ ).

**Conclusions:** In non-myopic eyes, the parapapillary gamma zone composed by external oblique border tissue was significantly associated with the disc ovality and disc rotations around vertical and horizontal axes. From a biomechanical perspective, parapapillary gamma zone may contribute to the optic disc stability in association with the structure of BMO.

**Keywords:** Gamma zone; beta zone; optic disc; Bruch's membrane opening (BMO); ovality index

Received: 11 April 2020; Accepted: 15 September 2020; Published: 15 December 2020.

doi: 10.21037/aes-20-88

View this article at: <http://dx.doi.org/10.21037/aes-20-88>

## Introduction

The funduscopy parapapillary beta zone defined by visible choroidal vessels and the sclera has been put forward for about 30 years (1). With the application of spectral domain optical coherence tomography (SD-OCT), the funduscopy beta zone has recently been divided into 2 subzones: gamma

zone and (new) beta zone (2,3). Parapapillary gamma zone was defined as the peripapillary region free of Bruch's membrane (BM), and the (new) parapapillary beta zone was defined by the continued presence of BM and absence of retinal pigment epithelial.

Several studies have shown that parapapillary beta zone

was associated with age and glaucoma, while parapapillary gamma zone was strongly correlated with axial myopia (3-5). It has been suggested that the development of gamma zone was related to a vertical optic disc rotation during axial elongation and the reduced risk of macular BM defect (6,7). However, gamma zone could be observed in hyperopic eyes, whose location and morphology seem to be different with those in myopic subjects. We hypothesized that factors other than axial myopia may be correlated with the onset and development of gamma zone. Therefore, we conducted this study to explore the microstructural features of parapapillary gamma zone and beta zone in non-myopic healthy eyes by using the enhanced depth imaging technology of SD-OCT. We present the following article in accordance with the STROBE guideline checklist (available at <http://dx.doi.org/10.21037/aes-20-88>).

## Methods

### Participants

The participants included were from the Shanghai Eye & ENT Hospital of Fudan University from June, 2017 to April, 2019. The participants included were required to have refractive error no less than -1 D, axial length less than 24.5 mm, and a best corrected visual acuity of 0.6 or more. Meanwhile, we excluded those with ophthalmic diseases (e.g., glaucoma, diabetic retinopathy) or history of refractive surgery. The study protocol was approved by the Institutional Ethics Committee. All subjects consented to participate before the ophthalmologic examinations were performed. The study protocol and data collection adhered to the tenets of the Declaration of Helsinki (as revised in 2003) and was approved by the Institutional Review Board of Shanghai Eye & ENT Hospital of Fudan University (2019-003). All study participants consented to the ophthalmologic examinations before they were performed.

### Data collection

All subjects underwent comprehensive ophthalmologic examinations, including visual acuity assessment, refractometry, intraocular pressure (IOP) measurement using Goldmann applanation tonometry, slit-lamp biomicroscopy. Other ocular parameters measurement included axial length, central cornea thickness, anterior chamber depth, etc. (Lenstar LS 900; Haag-Streit Diagnostics, USA), color photography of the optic nerve

head (CR-DGI; Canon, Inc., Tokyo, Japan) and SD-OCT (Spectralis OCT, Heidelberg Engineering, Heidelberg, Germany) scanning of the optic disc and fovea.

### *Determination of parapapillary beta zone and gamma zone*

Spectralis HRA + OCT system was used to scan the optic disc and peripapillary region. In the study, the whole optic disc and peripapillary region was captured in a  $15^\circ \times 15^\circ$  rectangle for horizontal scans. This rectangle was scanned with 37 B-scans, the distance between each section was 121  $\mu\text{m}$ . Meanwhile, we captured 24 radial lines B-scans in enhanced depth imaging mode with a B-scan angle of  $7.5^\circ$  to include the entire optic disc and peripapillary region. Both rectangular and radial scanning automatic real time (ART) modes were set to 24 images, and scans with quality score less than 15 were excluded from further measurement. In addition, operator would capture a single scan in 100 ART modes if not satisfied with the imaging quality.

Microstructure of peripapillary atrophy (PPA) area has been divided to alpha, beta and gamma zones (3). The alpha zone was characterized by the presence of BM covered by an irregular retinal pigment epithelium (RPE), while in beta zone BM was devoid of RPE cells, and gamma zone extended between the end of BM and the inner border of peripapillary ring as the optic disc border. The area of beta zone and gamma zone were measured by the measurement tools built in the Spectralis HRA + OCT software. Measurements were performed by a masked observer (D Zhuang).

### *Assessment of disc rotations around 3 axes and optic disc shape*

As described previously in detail (8), the optic disc rotation was divided around vertical axis, horizontal axis and sagittal axis. Rotations around the horizontal and vertical axis were calculated by trigonometry as the cosine of the ratio of horizontal and vertical diameters measured on the red-free fundus photographs to corresponding diameters measured on the OCT images. Sagittal rotation was measured directly on the red-free fundus photograph by the angle between the vertical axis and the longest disc diameter. The minimum and maximum diameters of optic disc and Bruch's membrane opening (BMO) were measured using the built-in tools on the SD-OCT image. Disc ovality index was calculated as the ratio of the minimum diameter to the maximum diameter of the optic disc. BMO ovality ratio

**Table 1** Main ocular parameters in gamma zone group and non-gamma zone group

| Variables                     | Non-gamma group (n=70) | Gamma group (n=62) | P value |
|-------------------------------|------------------------|--------------------|---------|
| Age (years)                   | 52.2±14.2              | 47.65±16.4         | 0.090   |
| Female, n (%)                 | 44 (62.9)              | 41 (66.1)          | 0.698   |
| Axial length (mm)             | 22.81±0.75             | 22.77±0.88         | 0.794   |
| Disc ovality index            | 0.91±0.06              | 0.84±0.07          | <0.001  |
| Vertical rotation (°)         | 5.94±2.59              | 9.38±3.10          | <0.001  |
| Horizontal rotation (°)       | 1.23±1.88              | 2.97±2.86          | <0.001  |
| Sagittal rotation (°)         | -11.74±23.31           | -14.21±30.57       | 0.600   |
| BMO ovality ratio             | 0.91±0.06              | 0.94±0.05          | <0.001  |
| Central cornea thickness (µm) | 539.65±28.97           | 551.39±31.34       | 0.034   |
| Aqueous depth (mm)            | 2.48±0.58              | 2.45±0.60          | 0.762   |
| Lens thickness (mm)           | 4.22±0.50              | 4.36±0.49          | 0.184   |

was calculated as the ratio of the minimum diameter to the maximum diameter of the BMO.

### Statistical analysis

SPSS 22.0 (IBM Corp., Armonk, NY, USA) was used for data analysis. Continuous variables were presented as means ± standard deviations, category variables as n (%). Student's t-test was used to evaluate data between two groups. Univariate analysis was performed to determine the correlations between the size of gamma and beta zone and major ocular parameters. Those parameters which showed significant associations in the univariate analysis were further included in multivariate linear regression analysis to explore the independent factor. Two-tailed  $P < 0.05$  was considered statistically significant.

### Results

A total of 132 healthy eyes from 71 subjects were included in this study. Mean age was 50.27±15.40 years (median, 53 years; range, 16–77 years). Mean axial length was 22.79±0.81 mm (median, 22.78 mm; range, 21.18–24.41 mm). All eyes were phakic.

Sixty-two eyes of 36 subject had a gamma zone, including 10 unilateral and 26 bilateral. There was no significant difference in age, sex, axial length, anterior chamber depth, and lens thickness between gamma zone group and control group ( $P > 0.05$ , Table 1). The presence of gamma zone was

associated with smaller disc ovality index ( $P < 0.001$ ), larger BMO ovality ratio ( $P < 0.001$ ), thicker cornea thickness ( $P = 0.014$ ) and larger rotation degree around vertical ( $P < 0.001$ ) and horizontal axes ( $P < 0.001$ ).

Among the eyes with gamma zone (Figure 1), 22 gamma zones were located at temporal region (35.5%), 22 gamma zones were at inferior region (35.5%) and 18 gamma zones were at nasal region (29.0%). Eyes in temporal gamma zone group had a longer axial length (23.67±0.70 vs. 22.34±0.65 mm,  $P < 0.001$ ), less disc ovality index (0.80±0.07 vs. 0.85±0.07,  $P = 0.013$ ), larger degree rotations around vertical axis (11.15°±2.96° vs. 8.31°±2.17°,  $P < 0.001$ ) and sagittal axis (2.44°±19.89° vs. -23.53°±31.81°,  $P = 0.002$ ) than those in non-temporal gamma zone group. BMO ovality ratio in eyes with a gamma zone was significantly larger than disc ovality index ( $P < 0.001$ ).

The average gamma zone area was 0.40±0.22 mm<sup>2</sup>. In univariate analysis, gamma zone area was significantly correlated with BMO ovality ratio ( $P = 0.037$ ), disc ovality index ( $P < 0.001$ ), central cornea thickness ( $P = 0.027$ ), the longest disc diameter ( $P = 0.004$ ), minimum BMO diameter ( $P < 0.001$ ) and maximum BMO diameter ( $P = 0.001$ ). In multivariate analysis, we dropped age ( $P = 0.103$ ), axial length ( $P = 0.248$ ), vertical rotation ( $P = 0.155$ ), horizontal rotation ( $P = 0.531$ ), sagittal rotation ( $P = 0.748$ ), aqueous depth ( $P = 0.578$ ), and the shortest disc diameter ( $P = 0.994$ ). Finally, gamma zone area was correlated with disc ovality index ( $P < 0.001$ , Figure 2) and longest disc diameter ( $P = 0.040$ , Table 2).

Fifty-five eyes of 36 subjects had a beta zone, including

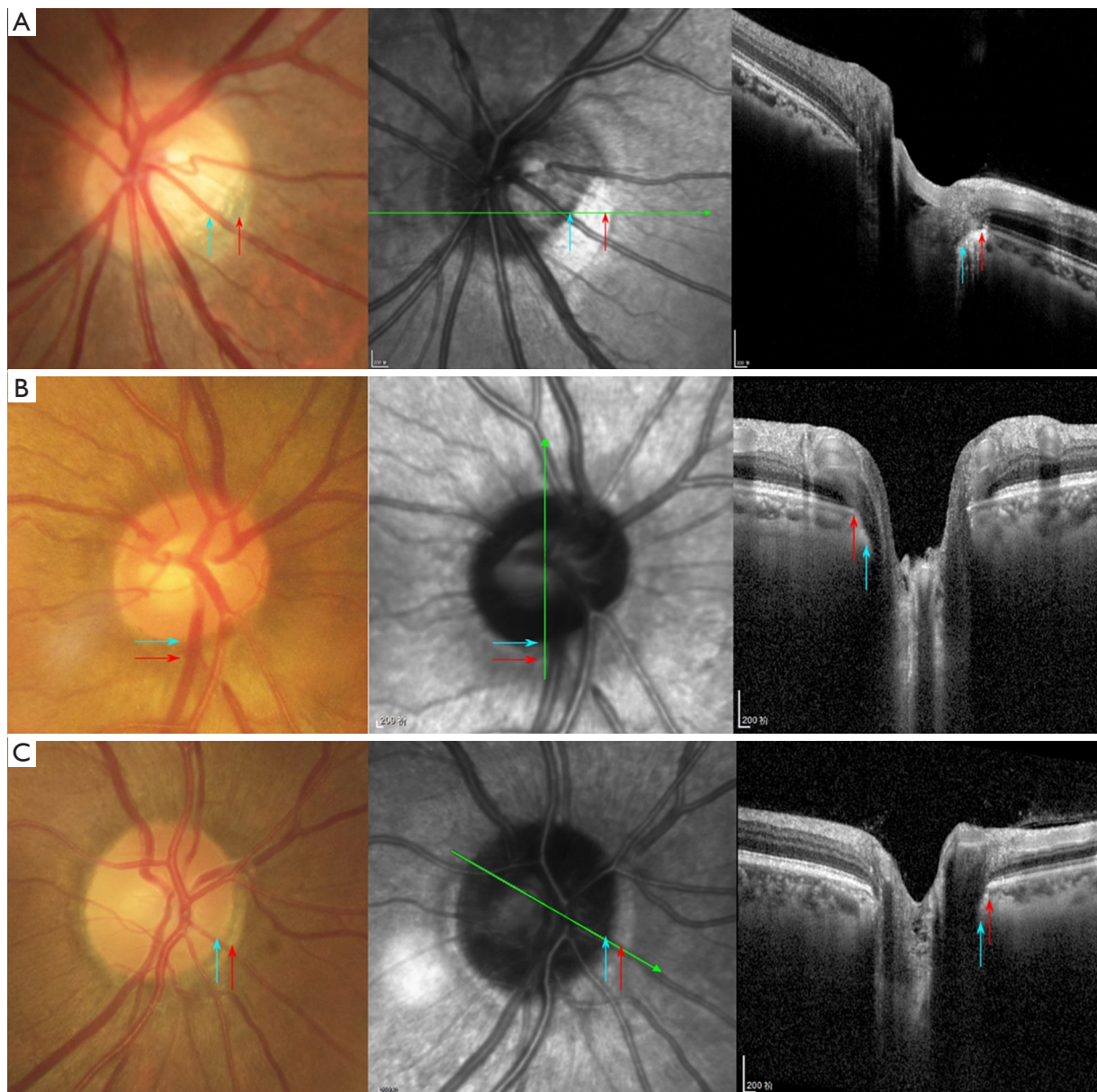


**Figure 1** Fundus photograph and OCT images of the parapapillary gamma zone (between blue arrow and red arrow) in the non-myopic eyes. The gamma zone, which is composed by externally oblique border tissue, could locate in temporal (A), inferior (B) and nasal (C) regions around disc in non-myopic eyes. 567 mm × 761 mm (72 × 72 DPI). Green arrows indicate location of the B-scan. OCT, optical coherent tomography.

17 unilateral and 19 bilateral. The presence of beta zone was only correlated with age ( $P < 0.001$ ). The rotation around all three axes was not significantly correlated with presence of beta zone, respectively ( $P > 0.05$ ). The average beta zone area was  $0.53 \pm 0.38 \text{ mm}^2$ . In univariate analysis, beta zone area was correlated with age ( $P = 0.007$ ), and sagittal rotation

( $P = 0.035$ ). In multivariate analysis, beta zone area was only associated with age ( $P = 0.015$ , *Table 2*). The disc ovality index in eyes with parapapillary beta zone did not have a significant difference compared to those without beta zone ( $P = 0.887$ ). Eyes with a beta zone showed no difference between BMO ovality ratio and disc ovality index ( $P = 0.120$ ).

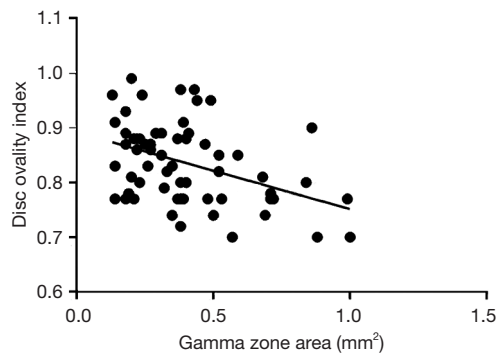


**Figure 2** Scatterplot showing the correlation between parapapillary gamma zone area and disc ovality index. 440 mm × 306 mm (144×144 DPI).

## Discussion

These results demonstrated that in non-myopic eyes, the parapapillary gamma zone located quite often in peripapillary inferior and nasal regions, other than temporal region. The presence of gamma zone was significantly correlated with the disc ovality index, BMO ovality ratio and disc rotations around vertical and horizontal axes. In eyes with gamma zone, the BMO ovality ratio was significantly higher than ovality index and closer to 1. While the presence and area of beta zone was only associated with age in non-myopic eyes, no significant relationship was found with disc rotation around 3 axes and ovality index.

Our findings revealed that the presence of gamma zone was associated with tilted discs in non-myopic eyes. A tilted optic disc was previously defined as a disc ovality index less than 0.75–0.80 according to fundus photos (9,10). In the current study, we further measured the disc diameters and disc rotation angles around 3 axes based on SD-OCT images, which could provide more accurate data about three-dimensional optic disc shape (8). Tilted optic discs have been reported as a morphologic feature associated with myopia (9–12). In myopic eyes, gamma zone was located most often in the temporal peripapillary region. It has been suggested that the development of gamma zone was associated with the reduced risk of macular BM defect during myopic axial elongation (7). In accordance with this notion, our data found that compared with the non-temporal gamma zone group, eyes with temporal gamma zone had a longer axial length and rotated more around vertical axis. However, gamma zone was often located in the nasal and inferior regions whose average axial length

of those eyes was 22.34 mm in our study, suggesting other factors may involve in the gamma zone development in non-myopic eyes. The interrelationship among the presence of gamma zone, the decreased disc ovality index, and the increased BMO ovality ratio, indicates the biomechanical role that parapapillary gamma zone may play in disc stability. It could be postulated that the shape of BMO tends to keep round to make structures strong in response to biomechanical influence around optic nerve head. If there is no gamma zone neighboring the tilted disc, the shape of the BMO would be not enough round and probably less stable.

The parapapillary gamma zone in non-myopic eyes appeared to be composed by externally oblique border tissue in SD-OCT images. Our data indicated that the length of externally oblique border tissue was strongly associated with the gamma zone area and disc ovality index. In myopic eyes, it may additionally include peripapillary elongated sclera flange as part of gamma zone (5,13). Anatomically, the optic nerve head is a three-layered foramen in the posterior region of the ocular globe. The first layer is BM, forming the papillary BM's opening. The second layer is the peripapillary choroid which opens up in the region of the optic nerve head. The deepest layer is formed by the peripapillary scleral flange and act as a biomechanical anchor for the lamina cribrosa (14). While BM simply ends at the border of BM opening, the edge of the peripapillary choroid and sclera flange is separated from the intrapapillary region by border tissue of Elschnig and Jacoby (15,16). The gamma zone and its underlying border tissue connecting between BM and the optic nerve pia mater may have importance for biomechanical stability of optic nerve head. It may also have potential importance for optic disc head related diseases, such as glaucoma. Previous reports have showed that gamma zone is related to the absence of glaucoma. The rate of glaucoma progression was slower for eyes with beta zone devoid of BM (equivalent to gamma zone) than for eyes with beta zone with intact BM (17,18). Further studies are needed to clarify whether gamma zone has a protective effect to on glaucomatous optic neuropathy and its mechanism.

The biomechanical stress of the border tissue may not be even in some tilted disc of non-myopic eyes, and then the gamma zone may develop to balance the stress and strain. The size of parapapillary gamma zone may serve as a sign of border tissue stretching. In extreme conditions, the biomechanical strength of border tissue may not be strong enough to bear the tension of optic nerve dura mater on the peripapillary region. Stretching of the border tissue

**Table 2** Linear regression analysis of variables associated with peripapillary gamma zone area and beta zone area

| Variable                    | Univariate analysis |                               | Multivariate analysis |                               |
|-----------------------------|---------------------|-------------------------------|-----------------------|-------------------------------|
|                             | P value             | Standardized coefficient beta | P value               | Standardized coefficient beta |
| <b>Gamma zone area</b>      |                     |                               |                       |                               |
| Age (years)                 | 0.103               | -0.209                        | -                     | -                             |
| Axial length, mm            | 0.248               | 0.149                         | -                     | -                             |
| Disc ovality index          | <0.001              | -0.547                        | <0.001                | -0.499                        |
| BMO ovality ratio           | 0.037               | 0.266                         | -                     | -                             |
| Vertical rotation (°)       | 0.155               | 0.183                         | -                     | -                             |
| Horizontal rotation (°)     | 0.531               | -0.081                        | -                     | -                             |
| Sagittal rotation (°)       | 0.748               | 0.042                         | -                     | -                             |
| Aqueous depth (mm)          | 0.578               | 0.077                         | -                     | -                             |
| Lens thickness (μm)         | 0.137               | -0.236                        | -                     | -                             |
| Longest disc diameter (μm)  | 0.004               | 0.367                         | 0.040                 | 0.270                         |
| Shortest disc diameter (μm) | 0.994               | -0.001                        | -                     | -                             |
| Maximum BMO diameter (μm)   | 0.001               | 0.435                         | -                     | -                             |
| Minimum BMO diameter (μm)   | <0.001              | 0.542                         | -                     | -                             |
| <b>Beta zone area</b>       |                     |                               |                       |                               |
| Age (years)                 | 0.007               | 0.236                         | 0.015                 | 0.256                         |
| Axial length (μm)           | 0.353               | -0.120                        | -                     | -                             |
| Disc ovality index          | 0.401               | 0.109                         | -                     | -                             |
| BMO ovality ratio           | 0.123               | -0.135                        | -                     | -                             |
| Vertical rotation (°)       | 0.113               | -0.203                        | -                     | -                             |
| Horizontal rotation (°)     | 0.975               | -0.004                        | -                     | -                             |
| Sagittal rotation (°)       | 0.035               | 0.184                         | -                     | -                             |
| Aqueous depth (mm)          | 0.605               | 0.072                         | -                     | -                             |
| Lens thickness (μm)         | 0.809               | -0.039                        | -                     | -                             |
| Longest disc diameter (μm)  | 0.146               | -0.190                        | -                     | -                             |
| Shortest disc diameter (μm) | 0.634               | -0.063                        | -                     | -                             |
| Maximum BMO diameter (μm)   | 0.113               | -0.207                        | -                     | -                             |
| Minimum BMO diameter (μm)   | 0.052               | -0.173                        | -                     | -                             |

BMO, Bruch's membrane opening.

of Elschnig and Jacoby may finally lead to the disruption of border tissue and the development of peripapillary intrachoroidal cavitations (19-21). It was evidenced by our previous findings that the eyes with peripapillary intrachoroidal cavitations had optic discs that were more spindle like configured mainly due to a disk rotation

around the vertical axis and around the sagittal axis (22). One thing to point out is that not all tilted optic disc has a gamma zone in our study, and differences in individual susceptibility to optic nerve head strain could be a possible explanation. Further studies are warranted to explore the biomechanical properties of the border tissue and how the

border tissues change parallel to other optic disc changes during adolescence.

There are several limitations to our study. First, this was a hospital-based research so that the prevalence of gamma zone and the prevalence of tilted discs in non-myopic eyes cannot be calculated, which might be much lower than those in myopic eyes. These values may be of importance to clarify the biomechanical role of the parapapillary gamma zone. Second, as a cross-sectional research, this study was unable to investigate the dynamic process of gamma zone formation. It also held true for tilted and rotated optic discs. The reported prevalence of tilted optic discs in adult was 3.5% in Tanjong Pagar study (9) and 1.6% in Blue Mountains study (11). However, there was no report on these values in infants and children. Previous longitudinal studies in children have showed that tilted disc and PPA may be an acquired feature in myopic eyes (23). As the myopic peripapillary tissue changed, the size and shape of the border tissue changed, whereas the BMO diameter remained relatively stable. Knowledge gained on the developmental change of optic disc and peripapillary region in emmetropic and hyperopic eyes will greatly help to understand the optic nerve head biomechanics.

In summary, our findings demonstrated that the presence of gamma zone was correlated with a more oval disc rotated around vertical and horizontal axes in non-myopic eyes. From a biomechanical perspective, parapapillary gamma zone and its underlying border tissue may contribute to optic disc stability in association with the structure of BMO. Future studies are warranted to address the role of parapapillary gamma zone involved in the susceptibility of glaucomatous optic neuropathy.

## Acknowledgments

*Funding:* Supported by the grants from Science and Technology Commission of Shanghai Municipality (No. 16411962000). The sponsor or funding organization had no role in the design or conduct of this research.

## Footnote

*Provenance and Peer Review:* This article was commissioned by the Guest Editor (Xiulan Zhang) for the series “Ophthalmology Clinical Research” published in *Annals of Eye Science*. The article has undergone external peer review.

*Reporting Checklist:* The authors have completed the STROBE reporting checklist. Available at <http://dx.doi.org/10.21037/aes-20-88>

*Data Sharing Statement:* Available at <http://dx.doi.org/10.21037/aes-20-88>

*Conflicts of Interest:* All authors have completed the ICMJE uniform disclosure form (available at <http://dx.doi.org/10.21037/aes-20-88>). The series “Ophthalmology Clinical Research” was commissioned by the editorial office without any funding or sponsorship. The authors have no other conflicts of interest to declare.

*Ethical Statement:* The authors are accountable for all aspects of the work in ensuring that questions related to the accuracy or integrity of any part of the work are appropriately investigated and resolved. The study protocol and data collection adhered to the tenets of the Declaration of Helsinki (as revised in 2003) and was approved by the Institutional Review Board of Shanghai Eye & ENT Hospital of Fudan University (2019-003). All study participants consented to the ophthalmologic examinations before they were performed.

*Open Access Statement:* This is an Open Access article distributed in accordance with the Creative Commons Attribution-NonCommercial-NoDerivs 4.0 International License (CC BY-NC-ND 4.0), which permits the non-commercial replication and distribution of the article with the strict proviso that no changes or edits are made and the original work is properly cited (including links to both the formal publication through the relevant DOI and the license). See: <https://creativecommons.org/licenses/by-nc-nd/4.0/>.

## References

1. Jonas JB, Nguyen XN, Gusek GC, et al. Parapapillary chorioretinal atrophy in normal and glaucoma eyes. I. Morphometric data. *Invest Ophthalmol Vis Sci* 1989;30:908-18.
2. Jonas JB, Jonas SB, Jonas RA, et al. Parapapillary atrophy: histological gamma zone and delta zone. *PLoS One* 2012;7:e47237.
3. Dai Y, Jonas JB, Huang HL, et al. Microstructure of Parapapillary Atrophy: Beta Zone and Gamma Zone. *Invest Ophthalmol Vis Sci* 2013;54:2013-8.

4. Kim M, Kim TW, Weinreb RN, et al. Differentiation of parapapillary atrophy using spectral-domain optical coherence tomography. *Ophthalmology* 2013;120:1790-7.
5. Yoo YJ, Lee E, Kim T. Intereye difference in the microstructure of parapapillary atrophy in unilateral primary open angle glaucoma. *Invest Ophthalmol Vis Sci* 2016;57:4187-93.
6. Jonas JB, Fang Y, Weber P, et al. Parapapillary gamma and delta zones in high myopia. *Retina* 2018;38:931-8.
7. Jonas JB, Wang YX, Zhang Q, et al. Parapapillary Gamma Zone and Axial Elongation-Associated Optic Disc Rotation: The Beijing Eye Study. *Invest Ophthalmol Vis Sci* 2016;57:396-402.
8. Dai Y, Jonas JB, Ling Z, et al. Ophthalmoscopic-perspectively distorted optic disc diameters and real disc diameters. *Invest Ophthalmol Vis Sci* 2015;56:7076-83.
9. How AC, Tan GS, Chan YH, et al. Population prevalence of tilted and torted optic discs among an adult Chinese population in Singapore. *Arch Ophthalmol* 2009;127:894-9.
10. Tay E, Seah SK, Chan SP, et al. Optic disk ovality as an index of tilt and its relationship to myopia and perimetry. *Am J Ophthalmol* 2005;139:247-52.
11. Vongphanit J, Mitchell P, Wang JJ. Population prevalence of tilted optic disks and the relationship of this sign to refractive error. *Am J Ophthalmol* 2002;133:679-85.
12. Hwang YH, Yoo C, Kim YY. Myopic optic disc tilt and the characteristics of peripapillary retinal nerve fiber layer thickness measured by spectral-domain optical coherence tomography. *J Glaucoma* 2012;21:260-5.
13. Strouthidis NG, Yang H, Reynaud JF, et al. Comparison of clinical and spectral domain optical coherence tomography optic disc margin anatomy. *Invest Ophthalmol Vis Sci* 2009;50:4709-18.
14. Jonas JB, Holbach L, Panda-Jonas S. Peripapillary ring: histology and correlations. *Acta Ophthalmol* 2014;92:e273-9.
15. Anderson DR. Ultrastructure of the optic nerve head. *Arch Ophthalmol* 1970;83:63-73.
16. Hayreh SS. Anatomy and physiology of the optic nerve head. *Trans Am Acad Ophthalmol Otolaryngol* 1974;78:OP240-54.
17. Kim YW, Lee EJ, Kim TW, et al. Microstructure of  $\beta$ -zone parapapillary atrophy and rate of retinal nerve fiber layer thinning in primary open-angle glaucoma. *Ophthalmology* 2014;121:1341-9.
18. Yamada H, Akagi T, Nakanishi H, et al. Microstructure of Peripapillary Atrophy and Subsequent Visual Field Progression in Treated Primary Open-Angle Glaucoma. *Ophthalmology* 2016;123:542-51.
19. Jonas JB, Dai Y, Panda-Jonas S. Peripapillary suprachoroidal cavitation, parapapillary gamma zone and optic disc rotation due to the biomechanics of the optic nerve dura mater. *Invest Ophthalmol Vis Sci* 2016;57:4373.
20. Wang X, Rumpel H, Lim WEH, et al. Finite element analysis predicts large optic nerve head strains during horizontal eye movements. *Invest Ophthalmol Vis Sci* 2016;57:2452-62.
21. Spaide RF, Akiba M, Ohno-Matsui K. Evaluation of peripapillary intrachoroidal cavitation with swept source and enhanced depth imaging optical coherence tomography. *Retina* 2012;32:1037-44.
22. Dai Y, Jonas JB, Ling Z, et al. Unilateral peripapillary intrachoroidal cavitation and optic disc rotation. *Retina* 2015;35:655-9.
23. Kim TW, Kim M, Weinreb RN, et al. Optic disc change with incipient myopia of childhood. *Ophthalmology* 2012;119:21-26.e1.

doi: 10.21037/aes-20-88

**Cite this article as:** Shang K, Zhuang D, Dai Y. Microstructural features of parapapillary gamma zone and beta zone in non-myopic eyes. *Ann Eye Sci* 2020;5:33.